ACS MEASUREMENT SCIENCE Au
AN OPEN ACCESS JOURNAL OF THE AMERICAN CHEMICAL SOCIETY

pubs.acs.org/measureau

Article

Tandem Mass Spectrometry as an Independent Method for Corroborating Fluorine-18 Radioactivity Measurements in Positron Emission Tomography

H. Umesha Shetty,* Cheryl L. Morse, and Victor W. Pike

Cite This: *ACS Meas. Sci. Au* 2022, 2, 370–376

Read Online

ACCESS | Metrics & More | Article Recommendations | Supporting Information

ABSTRACT: Positron emission tomography (PET) uses many tracers labeled with fluorine-18 ($t_{1/2}$ = 109.8 min; β^+ 97%) for quantitative imaging of biochemical and physiological processes in animal and human subjects. In PET methodology, the radioactivity in a dose of an ^{18}F-labeled tracer to be administered to a living subject is measured with a calibrated ionization chamber. This type of detector measures the radioactivity of a sample relative to those of certified amounts of longer-lived surrogate isotopes that are recommended for detector calibration. No alternative means for corroborating widely varying fluorine-18 radioactivity measurements from calibrated ionization chambers has been available. Here, we describe an independent nonradiometric method for this purpose. In this method, highly sensitive liquid chromatography–tandem mass spectrometry (LC–MS/MS) is used to quantify the relative masses of the radioactive isotopologue ([^{18}F]**1**) and the accompanying nonradioactive counterpart (carrier **1**) in an ^{18}F-labeled tracer preparation to give the mole ratio of [^{18}F]**1**. High-performance liquid chromatography (HPLC) with a mass-calibrated absorbance detection is used alongside to provide a separate measurement of the aggregate mass of all isotopologues. The radioactivity of the radiotracer is then derived in becquerels (Bq) from these two measurements, plus Avogadro's number and the decay constant of fluorine-18. For the chosen example [^{18}F]LSN3316612, the radioactivity values determined nonradiometrically and with a selected ionization chamber were in fair agreement. In addition, LC–MS/MS alone was found to provide an accurate measure of the half-life of fluorine-18.

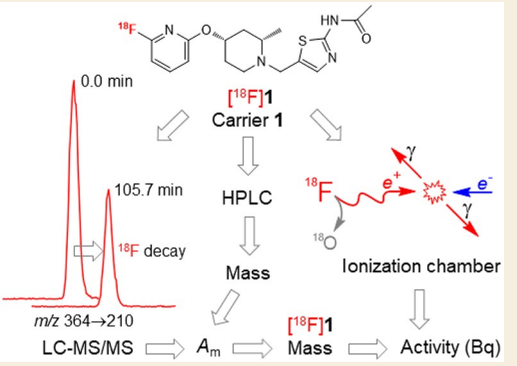

KEYWORDS: *fluorine-18, radioactivity, LC–MS/MS, radiotracer, molar activity, half-life*

INTRODUCTION

Positron emission tomography (PET) is an imaging technique that may be used with suitably designed radiotracers to measure enzymes, receptors, transporters, ion channels, and other macromolecules that govern biological processes in vivo.[1] As such, PET offers a valuable method for studying pathophysiology as well as for evaluating the pharmacokinetics and target occupancy by candidate molecules during clinical drug development.[2] Increasingly, PET is also used for medical diagnosis, especially in cancer.[3,4]

Many PET radiotracers are labeled with the radionuclide fluorine-18 because of its highly suitable decay characteristics. These include (i) almost total decay by positron emission (β^+ 96.86%, EC 3.14%), (ii) a useful half-life ($t_{1/2}$ = 109.8 min) that permits radiotracer distribution over distances that may be reached in a few hours from centralized radiopharmacies, and (iii) a low positron energy (0.635 MeV) that permits millimeter-level physical resolution from modern PET cameras. Moreover, the ability of fluorine to serve as a bioisostere for hydrogen and oxygen can be beneficially exploited in radiotracer design.[5] These advantages of fluorine-18 are especially exemplified in [^{18}F]2-deoxy-2-fluoro-D-glucose ([^{18}F]FDG), a radiotracer for measuring glucose metabolism, which finds broad diagnostic and biomedical research application in oncology and neurology.[6−9] The production of [^{18}F]FDG is commercialized and meets a market now exceeding one billion dollars. Other prominent examples of ^{18}F-labeled tracers with their imaging targets in parentheses are [^{18}F]FDOPA (brain dopaminergic neurons),[10] [^{18}F]fallypride (dopamine D_2 receptors),[11] [^{18}F]mefway (5-HT_{1A} receptors),[12] [^{18}F]FPEB (mGlu5 receptors),[13] and [^{18}F]florbetapir (amyloid-β plaque).[14] New PET radiotracer development is a highly active field.[15] For example, we have recently developed [^{18}F]LSN3316612 for imaging human brain *O*-linked β-*N*-acetyl glucosamine.[16]

Received: March 24, 2022
Revised: June 3, 2022
Accepted: June 6, 2022
Published: June 23, 2022

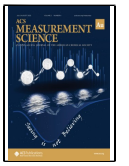

https://doi.org/10.1021/acsmeasuresciau.2c00018
ACS Meas. Sci. Au 2022, 2, 370–376

In PET methodology, an ionization chamber is used to measure the amount of radioactivity in a radiotracer dose, whereas a γ-counter and a PET camera are used to provide the time course of radioactivity in the subject's arterial blood and target tissue, respectively. These devices detect each pair of opposed 511 keV γ-rays that emerges upon the annihilation of an emitted positron with a nearby electron. The obtained radioactivity data should be accurate to ensure both subject radiation safety and the validity of quantitative outputs from PET experiments. Accuracy, however, depends on the calibration of the detectors.

Because direct calibration with short-lived isotopes such as fluorine-18 is not possible, ionization chambers must be calibrated with certified amounts of surrogate longer-lived γ-emitting isotopes. Most commonly, certified sources of ^{137}Cs ($t_{1/2}$ = 30.17 years; β^-, γ 662 keV) and ^{57}Co ($t_{1/2}$ = 271.79 days; ε, γ 122,136 keV) are available and recommended as secondary standards for this purpose. Even so, it is found that radioactivity measurements still vary quite considerably from one ionization chamber to another, even when the prescribed calibration method is uniformly applied.[17,18] Indeed, we have also observed substantial variations in measurements from several of our calibrated ionization chambers (see the Supporting Information). Therefore, a reliable and independent method for corroborating and referencing fluorine-18 radioactivity measurements from calibrated ionization chambers would be a welcome adjunct to PET methodology.

Radioactivity in becquerels, where one becquerel (Bq) is defined as one disintegration per second, is given by the product of the number of radiolabeled molecules and the decay constant of the radionuclide (λ), where $\lambda = \ln 2/t_{1/2}$. Thus, in principle, by measuring the mass of an ^{18}F-labeled tracer species in moles, its activity in Bq can then be calculated using Avogadro's number and the λ value for fluorine-18. Here, based on this principle, we describe our development of a nonradiometric LC−MS/MS method for measuring the radioactivity of an ^{18}F-labeled tracer and, for the first time, compare this type of radioactivity measurement with that from a calibrated ionization chamber. This method is possible because of the extraordinarily high mass sensitivity of modern LC−MS/MS instruments. We also used LC−MS/MS to measure the half-life of fluorine-18 for comparison with published values that have been determined radiometrically.

METHODS

Here, we summarize the rationale behind our experimental approach and describe the LC−MS/MS method for measuring an ^{18}F-labeled tracer. All other experimental methods are detailed in the Supporting Information.

Rationale Behind the Experimental Approach

An ^{18}F-labeled tracer preparation consists of the radioactive ^{18}F isotopologue plus the nonradioactive ^{19}F isotopologue in a physiologically acceptable medium, such as sterile saline. The ^{19}F isotopologue is unavoidably present in all PET radiotracer preparations obtained from all known radiochemical procedures and is known as the carrier.[15] The mass of the carrier isotopologue typically exceeds the mass of the ^{18}F isotopologue by about 2 orders of magnitude. The activity of a single radiotracer dose to be administered intravenously to a living human subject for a PET experiment is usually in the range of 100−200 MBq and is typically formulated within a small solution volume of about 10 mL. Thus, the carrier mass normally exists in the low nanomole range and at low concentrations. By use of sensitive liquid chromatography−tandem mass spectrometry (LC−MS/MS), we found it possible to measure the ratio of the relatively very low mass of radioactive isotopologue to the mass of the carrier isotopologue in representative ^{18}F-labeled tracer preparations. In this study, we exemplify this capability with [^{18}F]LSN3316612, which was being produced in our laboratory in very high radiochemical purity.[16] We show how this capability can be used for radioactivity determination.

The structures of LSN3316612 (**1**) and [^{18}F]LSN3316612 ([^{18}F]**1**) are shown in Figure 1. Also shown is the mass spectrometric

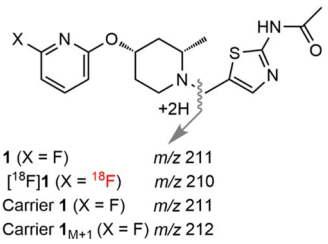

Figure 1. Structures of LSN3316612 (**1**; X = ^{19}F) and [^{18}F]-LSN3316612 ([^{18}F]**1**; X = ^{18}F). Also shown are the MS/MS generated product ions of **1** and constituent [^{18}F]**1** and carrier isotopologues in the radiotracer preparation.

fragmentation pattern that we obtained for **1**, which contains a single F-containing ion with the elemental composition $[C_{11}H_{16}N_2OF]^+$. We considered this fragment ion would be more suitable than the molecular ion for simultaneous LC−MS/MS measurement of both radioactive and nonradioactive isotopologues because of far less risk of possible contamination by other unknown ion sources. Concurrent fragment ion measurements readily provided the ratio of the mass of the [^{18}F]isotopologue (mass of [^{18}F]**1**) to that of the carrier (**1**) from which the mole fraction of [^{18}F]**1** was calculated as [[^{18}F]**1**]/([[^{18}F]**1** + [^{19}F]**1**]). These mole fraction values were then readily transformed into radiotracer molar activity values (A_m; ratio of radioactivity in becquerels to total mass in moles) by simple multiplication with the accepted decay constant for fluorine-18 (λ = 1.05214 × 10^{-4} per second) and Avogadro's number (N_A = 6.02214 × 10^{23} per mole) (eq 1). Multiplication of the A_m value of the sample by the total mass concentration of the radiotracer then provided a measurement of the radioactivity concentration of the sample.

$$A_m(\text{Bq/mol}) = [[\,^{18}\text{F}]\mathbf{1}]/([[\,^{18}\text{F}]\mathbf{1} + [^{19}\text{F}]\mathbf{1}]) \times \lambda \times N_A \quad (1)$$

In practice, for this study, the concentration of carrier **1** plus [^{18}F]**1** mass in a radiotracer preparation to be analyzed with LC−MS/MS was obtained with HPLC having an absorbance detector whose response had been calibrated for the concentration of **1** (see Supporting Information). Such a method was already conveniently available in our laboratory for the routine quality control of the radiotracer before release for PET study on a human subject.[16] In the absence of such a method, LC−MS/MS with an internal standard could be used for the same purpose. This approach might be preferred if the labeled compound to be measured has low UV absorbance.

We aimed to compare radioactivity values derived from the LC−MS/MS measurement of the sample A_m value and HPLC measurement of the sample concentration with those measured in a specified calibrated ionization chamber (dubbed ionization chamber E in the Supporting Information). In addition, the linearity, sensitivity, and accuracy of LC−MS/MS measurements of [^{18}F]**1** isotopologue were tested by following the radioactive decay of the radiotracer over two half-lives and using the data to compute the half-life of fluorine-18.

Measurement of [^{18}F]1 and Carrier 1$_{M+1}$, and the Ratio of Carrier 1$_{M+1}$ to Carrier 1 in Radiotracer Preparations

LC−MS/MS analyses of [^{18}F]**1** preparations were performed about 30 min after the end of each radiosynthesis. The radiotracer in saline was diluted 100-fold with acetonitrile/5 mM aq. ammonium acetate (50:50 v/v) in an autosampler vial. Samples (10 μL; ≤20 kBq) from the vial were injected 24 times onto LC−MS/MS at intervals of 10 min 30 s. LC−MS/MS analysis was performed with the setup

https://doi.org/10.1021/acsmeasuresciau.2c00018
ACS Meas. Sci. Au 2022, 2, 370−376

described in the Supporting Information to measure ions simultaneously from the transitions m/z 364 → 210 for [^{18}F]**1** and m/z 366 → 212 for carrier $\mathbf{1}_{M+1}$ in the radiotracer sample. The time of detection of [^{18}F]**1** in each case was determined by adding the LC retention time to the clock time of injection. Finally, after the elapse of 24 h, the decayed sample was analyzed once more with LC−MS/MS.

To determine the carrier $\mathbf{1}_{M+1}$ to carrier **1** ratio, the MS/MS was set up to monitor the m/z 365 → 211 transition for carrier **1** and the m/z 366 → 212 transition for carrier $\mathbf{1}_{M+1}$. The remaining sample in the autosampler vial was diluted 10-fold, and then a sample (10 μL) was injected onto the LC−MS/MS. The peak area ratio was measured for the product ions, m/z 212 for carrier $\mathbf{1}_{M+1}$ to m/z 211 for carrier **1**. The procedure was performed four times. A solution of reference **1** was similarly analyzed, and the peak area ratio was determined for the same two product ions. These ratios were used for converting the peak area of carrier $\mathbf{1}_{M+1}$ (measured) into that of carrier **1** peak area in the determination of A_m.

Calculation of A_m and Radioactivity from the Masses of [^{18}F]1 and Carrier

Following an LC−MS/MS analysis of [^{18}F]**1** preparation, as described above, the peak area of the carrier $\mathbf{1}_{M+1}$ was transformed to that of carrier **1** using the measured carrier $\mathbf{1}_{M+1}$ to carrier **1** ratio. The A_m of the radiotracer was then calculated from the [^{18}F]**1** peak area (A^*) and carrier **1** peak area (A) according to eq 2, using the values earlier defined for λ and N_A (eq 1).

$$A_m = (A^*/[A + A^*]) \times \lambda \times N_A \quad (2)$$

The A_m was calculated for each of the 24 analyses performed during the course of fluorine-18 decay. The natural logarithm of the molar activity ($\ln A_m$), without decay-correction, obtained from each injection was plotted against the respective time of detection of [^{18}F]**1** isotopologue by LC−MS/MS. The slope of the plot gave λ and thus a $t_{1/2}$ value for fluorine-18.

Additionally, A_m from each injection was decay-corrected to the time of the end of the radiosynthesis. This gave the mean ± SD of the A_m (GBq/μmol) value from 24 measurements with LC−MS/MS. HPLC analysis of 100 μL of the radiotracer preparation (Supporting Information) provided the combined mass concentrations of carrier **1** and [^{18}F]**1**. This mass (pmol) per volume was converted into the radioactivity data (kBq) per volume using the mean A_m value from 24 determinations.

RESULTS AND DISCUSSION

Background and Approach to LC−MS/MS Measurement of Radioactivity

We have earlier reported an LC−MS/MS method for measuring the constituent carbon-11 and carbon-13 isotopologues in ^{11}C-labeled tracer preparations as a basis for a nonradiometric method for measuring their molar activities.[19] Subsequently, we extended this nonradiometric approach into the development of a method to measure the arterial input function for a ^{11}C-labeled tracer being used for PET on human subjects.[20] In the method for measuring molar activity, the carrier$_{M+1}$ isotopologue (carbon-13 isotopologue plus natural abundance of ^{2}H and ^{17}O isotopologues) was measured to avoid the possible saturation of the MS/MS detector with the far more abundant carrier carbon-12 isotopologue during the concurrent measurement of the carbon-11 isotopologue. The LC−MS/MS peak area for carrier$_{M+1}$ isotopologue was accurately transformed to that of carbon-12 isotopologue using a separately measured carrier$_{M+1}$ to carbon-12 isotopologue ratio.

Similarly, in the method that we describe here, the radioactive and carrier isotopologues in an [^{18}F]**1** preparation (Figure 1) were each measured with LC−MS/MS and then used to determine the molar activity of the radiotracer. Once again, after accurately establishing the ratio of carrier M and M+1 isotopologues, the less abundant M+1 isotopologue was routinely measured concurrently with the radioactive isotopologue to avoid detector saturation. The determined ratio was then used to obtain the carrier M isotopologue value that would be used in radioactivity (Bq) determination, as described in Methods.

The theoretical carrier-free molar activity for fluorine-18 is the product of the decay constant and Avogadro's number and is exceedingly high (λN_A; 63348 GBq/μmol). Whereas the molar activity of [^{18}F]**1** produced in our laboratory (~76 ± 25 GBq/μmol)[16] has been quite similar to those typically reported for no-carrier-added ^{18}F-labeled tracers,[15] some laboratories have produced ^{18}F-labeled tracers with several-fold higher molar activity, such as [^{18}F]UCB-H with a molar activity of 815 GBq/μmol.[21] Clearly, there is no risk of detector saturation for such very high molar activity examples.

The signal-to-noise ratio for the LC−MS/MS detection of [^{18}F]**1** isotopologue was determined to be 109 at the time of measuring a molar activity of 13.8 GBq/μmol. The sensitivity of the MS/MS is therefore adequate for reliably measuring lower levels of molar activity. If the limit of quantification is considered to be the concentration at which the analyte can be detected with a signal-to-noise ratio of 10, then the deployed LC−MS/MS instrument can measure [^{18}F]**1** with a molar activity as low as 1.38 GBq/μmol. The limit of detection is the concentration of the analyte at which the signal-to-noise ratio is 3 to 1. Although not verified, the LC−MS/MS should be able to detect [^{18}F]**1** with a molar activity as low as 0.5 GBq/μmol. The dynamic range of quantification for our instrument is at least 10^4, and hence the method can be readily applied over the normal range of no-carrier-added ^{18}F-labeled tracer molar activities.

LC−MS/MS Method Development

Development of the LC−MS/MS method first required MS/MS fragmentation of reference **1** to identify a product ion that retained the fluorine atom. An MS/MS method then had to be set up to measure the radioactive and carrier isotopologues in [^{18}F]**1** samples. In a triple quadrupole MS/MS instrument (model API 5000, SCIEX), collision-induced dissociation of the $[M+H]^+$ ion (m/z 365) from reference **1** generated a dominant fluorine-containing product ion (m/z 211). This fragmentation reaction was deemed suitable for measuring carrier **1** along with [^{18}F]**1** (Figure 1). As observed with triple quadrupole MS/MS, the m/z 365→211 transition was also observed for **1** in an ion trap mass spectrometer (model Velos Pro; Thermo Fisher Scientific). This instrument, in its MS^3 settings, revealed further dissociation of the m/z 211 ion to give an m/z 98 ion, consistent with the fluorine-containing structure proposed for the m/z 211 ion (Supporting Information, Figures S3−S5). The instrument and compound-specific operating parameters (nebulizer, auxiliary, curtain, and collision activated dissociation (CAD) gases, source temperature, and electrospray and ion optics voltages) of the triple quadrupole MS/MS instrument were then optimized for the detection of the m/z 365 → 211 transition.

In the next step, the multiple reaction monitoring (MRM) table was edited to perform the transitions m/z 364 → 210 and m/z 366 → 212 for [^{18}F]**1** isotopologue and carbon-13 (plus natural abundances of ^{2}H/^{15}N/^{17}O) isotopologue (carrier $\mathbf{1}_{M+1}$), respectively, in [^{18}F]**1** samples (Figure 1). LC−MS/MS

https://doi.org/10.1021/acsmeasuresciau.2c00018
ACS Meas. Sci. Au 2022, 2, 370−376

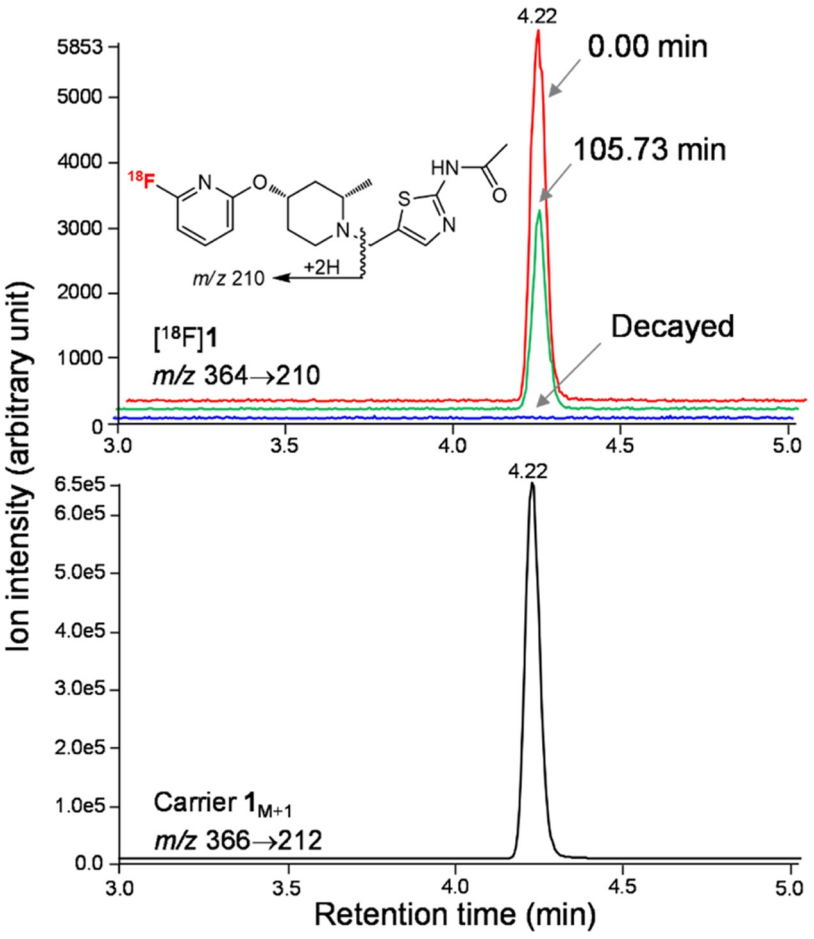

Figure 2. LC−MS/MS ion chromatograms from monitoring *m/z* 364 → 210 and *m/z* 366 → 212 transitions of [^{18}F]**1** and carrier $\mathbf{1}_{M+1}$ isotopologues, respectively, in a radiotracer preparation. The intensity of peak for [^{18}F]**1** decreased with ^{18}F decay, as shown with peaks at 0 min and after elapse of 105.73 min.

Table 1. Determination of A_m of [^{18}F]1 Preparation from the LC−MS/MS Data Alone

time (min)[a]	peak area of [^{18}F]**1**	peak area of carrier **1**[b]	area ratio[c]	A_m (GBq/μmol)[d]	A_m (GBq/μmol)[e]
0.0	1.3903×10^4	9.9070×10^6	1.4014×10^{-3}	88.77	109.9
52.9	9.2609×10^3	9.3875×10^6	9.8555×10^{-4}	62.43	107.9
116.4	6.1519×10^3	9.4221×10^6	6.5250×10^{-4}	41.33	106.7
169.2	4.6076×10^3	9.6676×10^6	4.7637×10^{-4}	30.18	108.7
222.1	3.2305×10^3	9.8724×10^6	3.2712×10^{-4}	20.72	104.3

[a]Time of detection of peaks of [^{18}F]**1** and carrier $\mathbf{1}_{M+1}$ for five injections starting with 0.0 min for the first injection. [b]Calculated peak area of carrier **1** from the measured peak area of carrier $\mathbf{1}_{M+1}$. [c]Ratio of peak area of [^{18}F]**1** to combined peak areas of carrier **1** and [^{18}F]**1**. [d]Derived from area ratio, decay constant of fluorine-18, and Avogadro's number. [e]Decay-corrected to end of synthesis.

analysis of reference **1** and of the carrier **1** from a fully decayed radiotracer preparation showed a peak for the transition *m/z* 366 → 212 but not for *m/z* 364 → 210, as was to be expected. This demonstrated that there is no cross-talk between these two sets of transitions during MS/MS acquisition.

As a further test of the lack of cross-talk, a diluted solution of an [^{18}F]**1** preparation was repeatedly injected onto LC−MS/MS at constant time intervals over a period of two half-lives of fluorine-18. At each time point, MS/MS detected the peak for [^{18}F]**1** and satisfactorily measured its area along with that of the $\mathbf{1}_{M+1}$ isotopologue. Figure 2 shows the LC−MS/MS peaks for [^{18}F]**1** and carrier $\mathbf{1}_{M+1}$ isotopologues generated from the transitions *m/z* 364 → 210 and *m/z* 366 → 212, respectively. The intensity of the [^{18}F]**1** peak diminished as time elapsed, in accord with fluorine-18 decay. Also, this peak was not detected in the radiotracer preparation after the sample had decayed for 24 h.

Another LC−MS/MS method was set up with transitions *m/z* 366 → 212 and *m/z* 365 → 211 for measuring carrier $\mathbf{1}_{M+1}$ and carrier **1** isotopologues, respectively, and thus their ratio in the [^{18}F]**1** preparation. The LC−MS/MS analysis performed with these transitions gave a $\mathbf{1}_{M+1}$ to **1** ratio of 0.12922 ± 0.00080 for carrier **1** in a radiotracer preparation and 0.13005 ± 0.00084 (mean ± SD; n = 6) for reference nonradioactive **1**. For comparison, the calculated $\mathbf{1}_{M+1}$ to **1** ratio based on natural abundances of ^{13}C/^{2}H/^{15}N/^{17}O in $[C_{11}H_{16}FN_2O]^+$ for the product ion *m/z* 211 is 0.12936. The measured and calculated ratios are effectively indistinguishable and verify that there is no alteration in the composition of

https://doi.org/10.1021/acsmeasuresciau.2c00018
ACS Meas. Sci. Au 2022, 2, 370−376

isotopologues in the carrier during the synthesis and purification of the radiotracer [^{18}F]**1**.

LC−MS/MS peak areas for carrier $\mathbf{1}_{M+1}$ were converted into those of carrier **1** using the carrier $\mathbf{1}_{M+1}$ to **1** ratio. Table 1 shows LC−MS/MS peak areas for [^{18}F]**1**, the derived peak areas for carrier **1**, and the calculated A_m values from five measurements (out of 24) performed over two half-lives of fluorine-18 for a single radiotracer preparation. The ratio of peak area for [^{18}F]**1** to the combined peak areas for carrier **1** and [^{18}F]**1** gave the mole fraction that was labeled with fluorine-18. Upon multiplying this peak area ratio with the decay constant of fluorine-18 ($\lambda = \ln 2/t_{1/2}$ where $t_{1/2}$ is taken to be 6588 s) and with Avogadro's number gave the molar activity (A_m) of the [^{18}F]**1** preparation. The calculated molar activity is shown at 0.0 min (the time of the detection of the first sample injected onto LC−MS/MS) and at four later time points for the same batch of radiotracer. The decrease in molar activity from 0.0 min to each of the four time points was consistent with the half-life of fluorine-18. Upon decay-correction to the end of radiotracer synthesis, the five sets of A_m values were highly comparable (107.5 ± 1.9 GBq/μmol; mean ± SD, n = 5).

LC−MS/MS Determination of the Half-Life of Fluorine-18

The linearity, sensitivity, and accuracy of LC−MS/MS detection for measuring low concentrations of the radiotracer were tested by determining the half-life of fluorine-18 from the time course for the decrease in mass of [^{18}F]**1** isotopologue. This involved measuring the decline in molar activity at specific time points during the decay of an [^{18}F]LSN3316612 sample over two half-lives. The logarithmic A_m values (GBq/μmol) were plotted against the clock time (first injection taken as 0.0 min) of LC−MS/MS detection of [^{18}F]**1** and carrier $\mathbf{1}_{M+1}$ isotopologues for 24 time points. Figure 3 is a

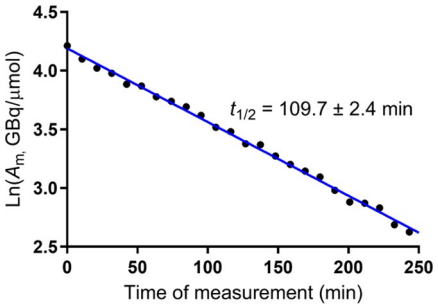

Figure 3. Plot of ln A_m of [^{18}F]**1** preparation measured with LC−MS/MS at 24 time points over a period of 243 min. The slope of the curve gave λ and thus the $t_{1/2}$ (109.73 ± 2.40 min; n = 6) for fluorine-18.

representative plot showing fluorine-18 decay as determined from the loss of mass of [^{18}F]**1** isotopologue in a radiotracer preparation. Plots from the LC−MS/MS analyses of six experiments gave the half-life for fluorine-18 as 109.73 ± 2.40 min (mean ± SD). This value is in very fair agreement with the most accepted values 109.72 ± 0.06 and 109.77 ± 0.018 that have been determined radiometrically.[22,23] Historically, all published half-lives for fluorine-18 have been determined radiometrically and have varied across the range 107 ± 4 to 114 ± 4 min.[22] The half-life determined here for fluorine-18 with LC−MS/MS has excellent accuracy, but we note that its precision is rather less than for the most accepted radiometrically determined values. We envisage scope to improve precision. Use of higher molar activity radiotracer samples would allow radioactive decay to be followed for a longer period to provide greater precision in plots of lnA_m versus time. Additionally, modern LC−MS/MS instrument with superior electronics and specificity (high-resolution MS) might be expected to improve the precision of ^{18}F and carrier isotopologue measurements.

Comparison of LC−MS/MS and an Ionization Chamber for Fluorine-18 Measurement

The LC−MS/MS measurement of [^{18}F]**1** and carrier $\mathbf{1}_{M+1}$ isotopologues in six radiotracer preparations gave A_m values of 97.89 ± 2.65, 90.39 ± 1.94, 76.58 ± 1.86, 107.68 ± 2.9, 74.39 ± 2.54, and 78.24 ± 2.09 GBq/μmol (decay-corrected to end of synthesis; mean ± SD; n = 24). These A_m values were derived from the mass concentration of [^{18}F]**1** isotopologue relative to that of carrier **1** isotopologue using Avogadro's number (N_A) and decay constant (λ) of fluorine-18, as in eq 1. Therefore, the activity (Bq) based on the mass of [^{18}F]**1** can be determined in a known volume of [^{18}F]**1** preparation by measuring the total concentration of carrier (**1**) and radiotracer ([^{18}F]**1**). The mass and radioactivity were measured by the procedure used for determining the molar activity of the radiotracer as part of its quality control before release for intravenous administration.[16]

In practice, for the HPLC method, a syringe filled with 100 μL of [^{18}F]**1** preparation was placed in an ionization chamber and measured for radioactivity. HPLC analysis with UV absorbance detection of the same radiotracer sample in the syringe provided the aggregate mass of carrier **1** and radiotracer [^{18}F]**1**. The total mass was converted into radioactivity data (Bq) using the A_m value measured with LC−MS/MS. Table 2 shows the mass-derived radioactivity

Table 2. Comparison of Radioactivity Data from Radiotracer's Mass (through LC−MS/MS and HPLC Measurements) with Those from Measurements in Ionization Chamber E

[^{18}F]**1** preparation	mass (pmol)[a]	LC−MS/MS (kBq)[b]	ionization chamber (kBq)[c]	difference (%)[d]
1	187.31	18,338	17,020	7.2
2	216.15	19,538	18,315	6.3
3	249.93	19,142	17,612	8.0
4	188.68	20,316	19,018	6.4
5	272.73	20,293	18,870	7.0
6	252.68	19,773	18,981	4.0

[a]Concentration of carrier **1** plus [^{18}F]**1**, measured by HPLC, in 100 μL of radiotracer preparation. [b]Activity data calculated from A_m and mass (pmol) measured by LC−MS/MS and HPLC, respectively. [c]Radioactivity in 100 μL of radiotracer preparation, measured in ionization chamber E (for comparison of radioactivity sensitivity of ionization chambers, see the Supporting Information). [d]Difference in kBq values based on the data from the LC−MS/MS method.

data (kBq) for six radiotracer preparations and the corresponding data from direct measurements using the ionization chamber. The radioactivity of [^{18}F]**1** preparation measured by the Biodex ionization chamber E was 6.5% ± 1.4% (n = 6) lower than that by the LC−MS/MS method. These comparative measurements, which were performed over a period of 6 months, revealed the good reproducibility of the technique.

https://doi.org/10.1021/acsmeasuresciau.2c00018
ACS Meas. Sci. Au 2022, 2, 370−376

The accuracy and precision of the measurements by an ionization chamber depend on the calibration procedure, in particular the dial settings,[17,24] used for the detector, as well as the radionuclidic purity, volume, and geometry of the sample.[25] The LC−MS/MS method described here is independent of such variables. Sources of error that might arise in this new method are in the construction of the calibration curve for HPLC determination of total mass and any radiochemical impurity in the radiotracer. A standardized balance with 0.01 mg sensitivity was used to prepare standard solutions of the tracer for the calibration curve in this study. The radiochemical purities of the six radiotracer preparations used in this study ranged from 98.4 to 99.0%, as determined by HPLC (see the Supporting Information). The impurity would be undetected by LC−MS/MS, leading to an underestimation of total radioactivity in the sample. By a similar consideration, this method is inapplicable to measuring the total radioactivity in ^{18}F-labeled compound mixtures. As shown in Table 2, the sets of radioactivity data obtained from LC−MS/MS and an ionization chamber are quite comparable. Consistent with this finding, in our prior study, the molar activity of a radiotracer labeled with another short-lived positron-emitter carbon-11 ($t_{1/2}$ = 20.4 min) measured with LC−MS/MS was also found to be very comparable with that measured with an ionization chamber.[19]

CONCLUSIONS

The LC−MS/MS method that we describe here can be used to corroborate fluorine-18 radioactivity values measured with calibrated ionization chambers, which, as we noted earlier, do not all give the same output measures, even when they are the same model and identically calibrated with the same surrogate isotope sources. This LC−MS/MS method avoids many of the sources of error in ionization chamber measurements and may have intrinsically higher accuracy and consistency. Therefore, the LC−MS/MS-based method might be used to normalize ionization chamber radioactivity measurements, especially among local sets of ionization chambers giving differing radioactivity values. The purpose of this method is in fact not for routine radioactivity measurements but for benchmarking and corroborating ionization chamber measurements. Nonetheless, the method should be applicable to all ^{18}F-labeled compounds that generate molecular or preferably fragment ^{18}F-containing ions, which are expected to be the vast majority of such compounds. Indeed, further elaboration of this method for regular benchmarking might use an organic compound that can be more easily labeled with fluorine-18 than compound **1**. We consider that this type of LC−MS/MS method has the potential to play a role in the improvement of both the consistency and accuracy of quantification in PET methodology.

ASSOCIATED CONTENT

Supporting Information

The Supporting Information is available free of charge at https://pubs.acs.org/doi/10.1021/acsmeasuresciau.2c00018.

Materials; safety; radiosynthesis of [^{18}F]**1**; comparison of calibrated ionization chambers for measurement of fluorine-18 radioactivity (Table S1); measurement of radioactivity by ionization chamber and mass by HPLC (Figures S1 and S2); fragmentation of $[M + H]^+$ of reference **1** and carrier **1** in an ion trap MS instrument (Figures S3 and S4); and LC−MS/MS settings for measuring [^{18}F]**1** and carrier $\mathbf{1}_{M+1}$ isotopologues (Figure S5) (PDF)

AUTHOR INFORMATION

Corresponding Author

H. Umesha Shetty − *Molecular Imaging Branch, National Institute of Mental Health, National Institutes of Health, Bethesda, Maryland 20892, United States;* orcid.org/0000-0002-5416-2940; Phone: 301-451-3923; Email: shettyu@mail.nih.gov; Fax: 301-480-5112

Authors

Cheryl L. Morse − *Molecular Imaging Branch, National Institute of Mental Health, National Institutes of Health, Bethesda, Maryland 20892, United States*

Victor W. Pike − *Molecular Imaging Branch, National Institute of Mental Health, National Institutes of Health, Bethesda, Maryland 20892, United States;* orcid.org/0000-0001-9032-2553

Complete contact information is available at: https://pubs.acs.org/10.1021/acsmeasuresciau.2c00018

Author Contributions

H.U.S. performed LC−MS/MS experiments. C.L.M. carried out radiosynthesis and radiochemical measurements. H.U.S. and V.W.P. designed the study and wrote the manuscript. All authors reviewed the manuscript.

Notes

The authors declare no competing financial interest.

ACKNOWLEDGMENTS

The unlabeled compound **1** and the precursor for the synthesis of [^{18}F]**1** were provided by Eli Lilly and Company (Indianapolis, IN). For radiosynthesis, fluorine-18 was produced by NIH Clinical PET Department (Chief, Dr. P. Herscovitch). The authors are also grateful to W. H. Miller for technical assistance. This study was funded by the Intramural Research Program of the National Institute of Mental Health, National Institutes of Health (IRP-NIMH-NIH: ZIA-MH002793).

REFERENCES

(1) Phelps, M. E. Positron emission tomography provides molecular imaging of biological processes. *Proc. Natl. Acad. Sci. U.S.A.* **2000**, *97*, 9226−9233.

(2) Ghosh, K. K.; Padmanabhan, P.; Yang, C.-T.; Ng, D. C. E.; Palanivel, M.; Mishra, S.; Halldin, C.; Gulyás, B. Positron emission tomographic imaging in drug discovery. *Drug Discovery Today* **2022**, *27*, 280−291.

(3) Pruis, I. J.; van Dongen, G. A. M. S.; Veldhuijzen van Zanten, S. E. M. The added value of diagnostic and theranostic PET imaging for the treatment of CNS tumors. *Int. J. Mol. Sci.* **2020**, *21*, 1029.

(4) Unterrainer, M.; Eze, C.; Ilhan, H.; Marschner, S.; Roengvoraphoj, O.; Schmidt-Hegemann, N. S.; Walter, F.; Kunz, W. G.; Munck af Rosenschöld, P.; Jeraj, R.; Albert, N. L.; Grosu, A. L.; Niyazi, M.; Bartenstein, P.; Belka, C. Recent advances of PET imaging in clinical radiation oncology. *Radiat. Oncol.* **2020**, *15*, No. 88.

(5) Pike, V. W. Considerations in the development of reversibly binding PET radioligands for brain imaging. *Curr. Med. Chem.* **2016**, *23*, 1818−1869.

(6) Som, P.; Atkins, H. L.; Bandoypadhyay, D.; Fowler, J. S.; MacGregor, R. R.; Matsui, K.; Oster, Z. H.; Sacker, D. F.; Shiue, C. Y.; Turner, H.; Wan, C-N.; Wolf, A. P.; Zabinski, S. V. A fluorinated

glucose analog, 2-fluoro-2-deoxy-D-glucose (F-18): nontoxic tracer for rapid tumor detection. *J. Nucl. Med.* **1980**, *21*, 670−675.
(7) Hustinx, R.; Bénard, F.; Alavi, A. Whole-body FDG-PET imaging in the management of patients with cancer. *Semin. Nucl. Med.* **2002**, *32*, 35−46.
(8) Herholz, K.; Heiss, W.-D. Positron emission tomography in clinical neurology. *Mol. Imaging Biol.* **2004**, *6*, 239−269.
(9) Newberg, A.; Alavi, A.; Reivich, M. Determination of regional cerebral function with FDG-PET imaging in neuropsychiatric disorders. *Semin. Nucl. Med.* **2002**, *32*, 13−34.
(10) Gjedde, A.; Reith, J.; Dyve, S.; Léger, G.; Guttman, M.; Diksic, M.; Evans, A.; Kuwabara, H. Dopa decarboxylase activity of the living human brain. *Proc. Natl. Acad. Sci. U.S.A.* **1991**, *88*, 2721−2725.
(11) Mukherjee, J.; Yang, Z.-Y.; Das, M. K.; Brown, T. Fluorinated benzamide neuroleptics−III. Development of (*S*)-*N*-[(1-allyl-2-pyrrolidinyl)methyl]-5-(3-[^{18}F]fluoropropyl)-2,3-dimethoxybenzamide as an improved dopamine D-2 receptor tracer. *Nucl. Med. Biol.* **1995**, *22*, 283−296.
(12) Hillmer, A. T.; Wooten, D. W.; Bajwa, A. K.; Higgins, A. T.; Lao, P. J.; Betthauser, T. J.; Barnhart, T. E.; Rowley, H. A.; Stone, C. K.; Johnson, S. C.; Mukherjee, J.; Christian, B. T. First-in-human evaluation of ^{18}F-Mefway, a PET radioligand specific to serotonin-1A receptors. *J. Nucl. Med.* **2014**, *55*, 1973−1979.
(13) Wong, D. F.; Waterhouse, R.; Kuwabara, H.; Kim, J.; Brašić, J. R.; Chamroonrat, W.; Stabins, M.; Holt, D. P.; Dannals, R. F.; Hamill, T. G.; Mozley, P. D. ^{18}F-FPEB, a PET radiopharmaceutical for quantifying metabotropic glutamate 5 receptors: a first-in-human study of radiochemical safety, biokinetics, and radiation dosimetry. *J. Nucl. Med.* **2013**, *54*, 388−396.
(14) Wong, D. F.; Rosenberg, P. B.; Zhou, Y.; Kumar, A.; Raymont, V.; Ravert, H. T.; Dannals, R. F.; Nandi, A.; Brašić, J. R.; Ye, W.; Hilton, J.; Lyketsos, C.; Kung, H. F.; Joshi, A. D.; Skovronsky, D. M.; Pontecorvo, M. J. In vivo imaging of amyloid deposition in Alzheimer's disease using the novel radioligand [^{18}F]AV-45 (florbetapir F 18). *J. Nucl. Med.* **2010**, *51*, 913−920.
(15) Siméon, F. G.; Telu, S.; Cai, L.; Lu, S.; Pike, V. W. Fluorine-18 Radiochemistry for PET Imaging Applications − Fundamentals and Recent Advances. In *The Chemistry of Organofluorine Compounds. Patai's Chemistry of Functional Groups* Gouverneur, V.; Gandelman, M.; Marek, I., Eds.; John Wiley and Sons: London, 2022.
(16) Lu, S.; Haskali, M. B.; Ruley, K. M.; Dreyfus, N.J.-F.; DuBois, S. L.; Paul, S.; Liow, J.-S.; Morse, C. L.; Kowalski, A.; Gladding, R. L.; Gilmore, J.; Mogg, A. J.; Morin, S. M.; Lindsay-Scott, P. J.; Ruble, J. C.; Kant, N. A.; Shcherbinin, S.; Barth, V. N.; Johnson, M. P.; Cuadrado, M.; Jambrina, E.; Mannes, A. J.; Nuthall, H. N.; Zoghbi, S. S.; Jesudason, C. D.; Innis, R. B.; Pike, V. W. PET ligands [^{18}F]LSN3316612 and [^{11}C]LSN3316612 quantify *O*-linked-*β*-*N*-acetyl-glucosamine hydrolase in the brain. *Sci. Transl. Med.* **2020**, *12*, No. eaau2939.
(17) Bergeron, D. E.; Cessna, J. T.; Coursey, B. M.; Fitzgerald, R.; Zimmerman, B. E. A review of NIST primary activity standards for ^{18}F: 1982 to 2013. *J. Res. Natl. Inst. Stand. Technol.* **2014**, *119*, 371−396.
(18) Fitzgerald, R.; Zimmerman, B. E.; Bergeron, D. E.; Cessna, J. C.; Pibida, L.; Moreira, D. S. A new NIST primary standardization of ^{18}F. *Appl. Radiat. Isot.* **2014**, *85*, 77−84.
(19) Shetty, H. U.; Morse, C. L.; Zhang, Y.; Pike, V. W. Characterization of fast-decaying PET radiotracers solely through LC-MS/MS of constituent radioactive and carrier isotopologues. *EJNMMI Res.* **2013**, *3*, No. 3.
(20) Shetty, H. U.; Zoghbi, S. S.; Morse, C. L.; Kowalski, A.; Hirvonen, J.; Innis, R. B.; Pike, V. W. Development of a non-radiometric method for measuring the arterial input function of a ^{11}C-labeled PET radiotracer. *Sci. Rep.* **2020**, *10*, No. 17350.
(21) Warnier, C.; Lemaire, C.; Becker, G.; Zaragoza, G.; Giacomelli, F.; Aerts, J.; Otabashi, M.; Bahri, M. A.; Mercier, J.; Plenevaux, A.; Luxen, A. Enabling efficient positron emission tomography (PET) imaging of synaptic vesicle glycoprotein 2A (SV2A) with a robust and one-step radiosynthesis of a highly potent ^{18}F-labeled ligand ([^{18}F]UCB-H). *J. Med. Chem.* **2016**, *59*, 8955−8966.
(22) Mahony, J. D.; Markowitz, S. S. The half-life of fluorine-18. *J. Inorg. Nucl. Chem.* **1964**, *26*, 907−910.
(23) Unterweger, M. P.; Fitzgerald, R. Update of NIST half-life results corrected for ionization chamber source-holder instability. *Appl. Radiat. Isot.* **2014**, *87*, 92−94.
(24) Zimmerman, B. E.; Kubicek, G. J.; Cessna, J. T.; Plascjak, P. S.; Eckelman, W. C. Radioassays and experimental evaluation of dose calibrator settings for ^{18}F. *Appl. Radiat. Isot.* **2001**, *54*, 113−122.
(25) Cessna, J. T.; Schultz, M. K.; Leslie, T.; Bores, N. Radionuclide calibrator measurements of ^{18}F in a 3 ml plastic syringe. *Appl. Radiat. Isot.* **2008**, *66*, 988−993.

https://doi.org/10.1021/acsmeasuresciau.2c00018
ACS Meas. Sci. Au 2022, 2, 370−376